

6 Referências Bibliográficas

- 1 Capelli, Raffaella et al. **Organic light-emitting transistors with an efficiency that outperforms the equivalent light-emitting diodes.** Nature Materials 9, p. 496-503, 2010.
- 2 Daniel, T. Simon et al. **Organic electronics for precise delivery of neurotransmitters to modulate mammalian sensory function.** Nature Materials 8, p. 742-746, 2009.
- 3 Allison, R.R. et al. **Bio-nanotechnology and photodynamic therapy - State of the art review.** Photodiagnosis and Photodynamic Therapy 5, p. 19-28, 2008.
- 4 Epstein, Arthur. **Foreword.** Synthetic Metals 125, p.1, 2002.
- 5 Coropceanu, V. et al. **Charge Transport in Organic Semiconductors.** Chemical Review 107, p. 926-952, 2007.
- 6 Heck, B. et al. **A law controlling polymer recrystallization showing up in experiments on s-polypropylene.** Polymer, 48, p. 1352-1359, 2007.
- 7 Nardes, A. M., Dissertação de Mestrado, Technische Universiteit Eindhoven, 2007.
- 8 Montero, J. M. e Bisquert, J., Solid-State Electronics 55, p. 1-4, 2011.
- 9 A. Irfan et al., Journal of Molecular Structure 850, p. 79-83, 2008.
- 10 Chen, B.J. et al. **Electron drift mobility and electroluminescent efficiency of tris(8-hydroxyquinolinolato) aluminum.** Applied Physics Letters 75, p. 4010, 1999.
- 11 Ji, W. et al. **High-color-rendering flexible top-emitting warm-white organic light emitting diode with a transparent multilayer cathode.** Organic Electronics 12, p. 1137-1141, 2011.
- 12 Patricia, Freitag et al. **White top-emitting organic light-emitting diodes with forward directed emission and high color quality.** Organic Electronics 11, p. 1676-1682, 2010.

- 13 Park, S. H. et al. **Bulk heterojunction solar cells with internal quantum efficiency approaching 100%**. Nature Photon 3, p. 297-303, 2009.
- 14 Melzer, C. e Seggern, H., Enlightened organic transistors. Organic electronics 9, p. 470-472, 2010.
- 15 <http://jet.samsungmobile.com/>
- 16 Teixeira, K. C., Dissertação de Mestrado, PUC-Rio, 2010.
- 17 Quirino, W. et al. **White OLED using β -diketones rare earth binuclear complex as emitting layer**. Thin Solid Films 494, p. 23-27, 2006.
- 18 Thomson, Willam. Proceedings of the Royal Society of London 8 p.546-550, 1856.
- 19 Moodera, J.S. et al. **Large Magnetoresistance at Room Temperature in Ferromagnetic Thin Film Tunnel Junctions**. Physical Review Letters 74, p. 3273, 1995.
- 20 A., Fert et al. **Giant Magnetoresistance of (001)Fe/(001)Cr Magnetic Superlattices**. Physical Review Letters 61, p. 2472, 1988.
- 21 Kalinowski, J. et al. **Magnetic field effects on emission and current in Alq3-based electroluminescent diodes**. Chemical Physics Letters 380, p. 710-715, 2003.
- 22 Jullière, M. et al. **Tunneling between ferromagnetic films**. Physics Letters A 54, p. 225-226, 1975.
- 23 P. Grünberg et al. **Enhanced magnetoresistance in layered magnetic structures with antiferromagnetic interlayer exchange**. Physical Review B 39, p. 4828, 1989.
- 24 Arthur Epstein, Synthetic Metals 125, 1, 2001.
- 25 Ehrenreich, H. and Spaepen, F., Solid State Physics 56, p. 113-237, 2001.
- 26 Huicong, Q., Advanced E & M, p. 1-6, 2008.
- 27 B., Dieny et al. **Giant magnetoresistive in soft ferromagnetic multilayers**. Physical Review B 43, p. 1297, 1991.
- 28 D.L., Zhang et al. **Effect of nano-oxide layers on giant magnetoresistance in pseudo-spin-valves using Co2FeAl electrodes**. Journal of Magnetism and Magnetic Materials 323, p. 631-634, 2010.
- 29 Fowler, R. H. e Nordheim, L., Proceedings of The Royal Society A, 119, p. 173, 1928.

-
- 30 Ouerghemmi, H. B., et al. **Self-assembled monolayer effect on the characteristics of organic diodes.** Synthetic Metals 159, p. 551-555, 2009.
- 31 Dexter, D. L., The Journal of Chemical Physics 21,5, p. 836, 1953.
- 32 Förster, T., 10th Spiers Memorial Lecture, p. 7-17, 1959.
- 33 Sá, G. F. et al. **Spectroscopic properties and design of highly luminescent lanthanide coordination complexes.** Coordination Chemistry Reviews, 196, p. 165-195, 2000.
- 34 Prigodin, V. N., Synthetic Metals 156, p. 757-761, 2006.
- 35 Hu, B. e Wu, Y., Nature Materials 6, p. 985, 2007.
- 36 Wagemans, W. et al. **A two-site bipolaron model for organic magnetoresistance.** Journal of Applied Physics 103, 07F303, 2008.
- 37 Wohlgenannt, M. et al. **Bipolaron Mechanism for Organic Magnetoresistance.** Physical Review Letters 99, 216801, 2007.
- 38 Lampert, M.A. e Mark, P. (Eds.), Current Injection in Solids, Academic Press, 1970.
- 39 Wu, Y. et al. **Tuning magnetoresistance and magnetic-field-dependent electroluminescence through mixing a strong-spin-orbital-coupling molecule and a weak-spin-orbital-coupling polymer.** Physical Review B 75, 035214, 2007.
- 40 Wohlgenannt, M. et al. **Large magnetoresistance in nonmagnetic π -conjugated semiconductor thin film devices.** Physical Review B 72, 205202, 2005.
- 41 Heeger, A. J. et al. **Solitons in conducting polymers.** Review of Modern Physics 60, 781, 1988.
- 42 Sasaki, C. A., Dissertação de Mestrado, Escola Politécnica, USP, 1989.
- 43 Othman, M. K. et al., **ICSE2006 Proc.** 2006.
- 44 Yamaguchi, M. e Nagano, T., Thin Solid Films 363, 21, 2001.
- 45 Wu, Z. et al. **Improved efficiency of organic light-emitting devices employing bathocuproine doped in the electron-transporting layer.** Semiconductor Science Technology 18, 2003.
- 46 Sun Q. J. et al. **White light from polymer light-emitting diodes: Utilization of fluorenone defects and exciplex.** Applied Physics Letters 88, 163510, 2006.

-
- 47 Legnani, C. et al. **Organic light emitting diodes based on dipyridamole drug.** Thin Solid Films 515, P. 902-906, 2006.
- 48 Jun-Song, C. et al. **Organic Light-Emitting Diodes with Magnesium Doped CuPc as an Efficient Electron Injection Layer.** Chinese Physics Letters 25, p.719-721, 2008.
- 49 J. P. McKlevey, Solid State and Semiconductor Physics, Harpers & Row, NY, 1966.
- 50 Kahlert, H. e Seiler, D. G., Review of Scientific Instruments 48, 8, 1977.
- 51 Wohlgenannt, M. et al. **Magnetic field-effects in bipolar, almost hole-only and almost electron-only tris-(8-hydroxyquinoline) aluminum devices.** Physical Review B 77, 235209, 2008.
- 52 Koopmans B. et al. **Frequency dependence of organic magnetoresistance.** Applied Physics Letters 97, 123301, 2010.
- 53 Leonardo, C. R., Desenvolvimento de um Amplificador *Lock-in* com DSP operando em Altas Frequências, Dissertação de Mestrado, CBPF, 2008.
- 54 Sheng, Y. et al. **Effect of spin-orbit coupling on magnetoresistance in organic semiconductors.** Physical Review B 75, 035202, 2007.

Apêndice I

Durante este trabalho de mestrado outros trabalhos foram desenvolvidos e como fruto, os seguintes artigos foram publicados:

- Quirino, W. G.; Legnani, C.; dos Santos, R. M. B.; Teixeira, K. C.; Cremona, M.; Guedes, M. A.; Brito, H. F., “Electroluminescent devices based on rare-earth tetrakis β -diketonate complexes”, *Thin Solid Films* 517, p. 1096 -110, 2008.
- Marulanda, J. I., Cremona, M., Santos, R. M. B., Carvalho, M. C. R., Demenicis, L. S., “Characterization of SrTiO₃ thin films at microwave frequencies using coplanar waveguide linear resonator method”, *Microwave and Optical Technology Letters* 53, p. 2418-2422, 2011.

Com relação ao trabalho desenvolvido, estão sendo preparados dois artigos referentes aos resultados dos estudos:

- do comportamento da MR, nos dispositivos orgânicos produzidos, como função de diferentes materiais utilizados na camada transportadora de buracos.
- de investigação da MR sobre os dispositivos orgânicos produzidos baseados nos complexos de íons de terras-raras.

Apêndice II

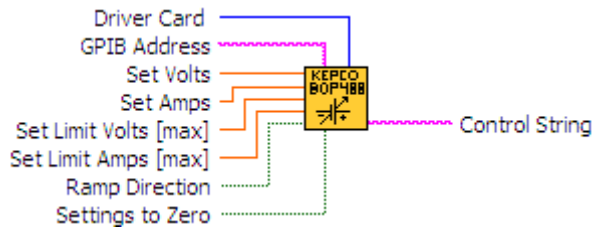
O tratamento realizado sobre os dados coletados a partir da detecção do amplificados *Lock-in* é realizado utilizando a seguinte rotina do software MatLab, construída durante este trabalho de mestrado.

```
clear
r=load('nome do arquivo.txt'); % dados coletados pelo Lock-in
B=r(:,1)*1e-3; % conversão do campo em Tesla
dV=r(:,2)*1e-6; % conversão dos dados coletados pelo lock-in em V
dI=dV/10e3; % dividir pela resistência 10k
dIdB=dI*10e6/5e-3; % multiplicar por 106 e dividir por dB (em T)
figure(1)
plot(B*1e3,dIdB,'o-') %construção do gráfico dI/dB em função de B
dIdB=dIdB+2
xlabel('Applied field (mT)')
ylabel('dI/dB (\muA/T)')
fit1 = fit(B,dIdB,'pchipinterp');
DI = integrate(fit1,B,B(1)); %integral da curva no gráfico dI/dB
I0=50; % media da corrente no dispositivo em \mu A
figure(2)
B=B*1E3;
DI=(-100)*(min(DI/I0)-DI/I0);
dados=[B,DI];
save DI_nome do arquivo.txt dados -ascii;
plot(B,DI,'o-') % construção do gráfico \Delta I/I0 (%) em função de B
xlabel('Applied field (mT)')
ylabel('\Delta I/I0 (%)')
grid
```

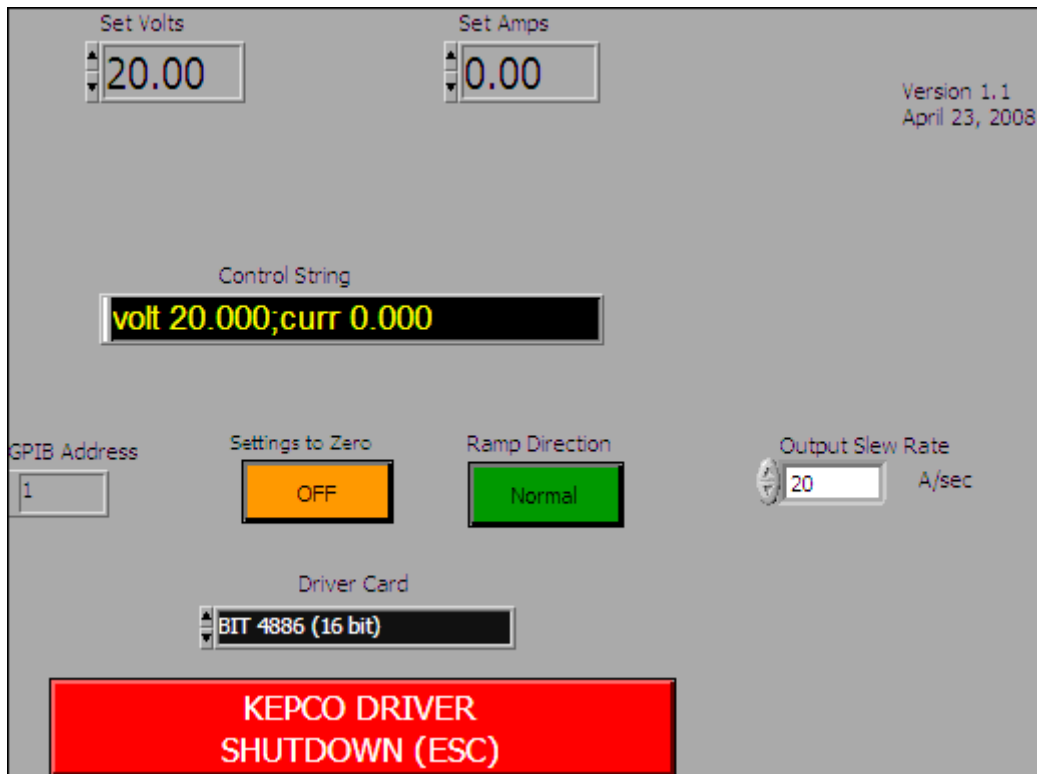
Apêndice III

O controle da fonte de corrente do eletroímã (i) e do amplificador *Lock-in* (ii), utilizados no sistema de medições, é feito remotamente através das rotinas do software Labview apresentadas abaixo. Uma das rotinas de Labview foram obtidas na aquisição do eletroímã e a outra foi obtida através do site da *Signal Recovery*:

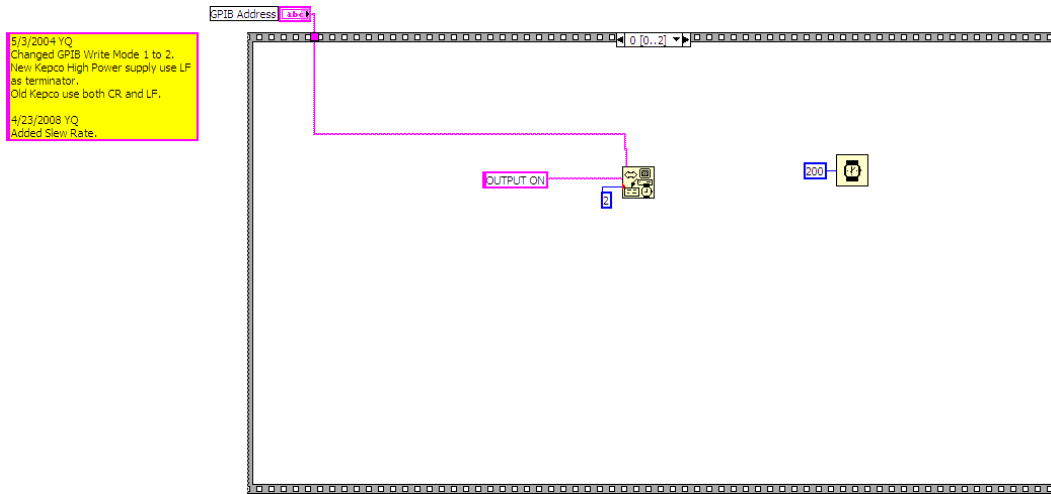
- (i) Controle da fonte de corrente do eletroímã:



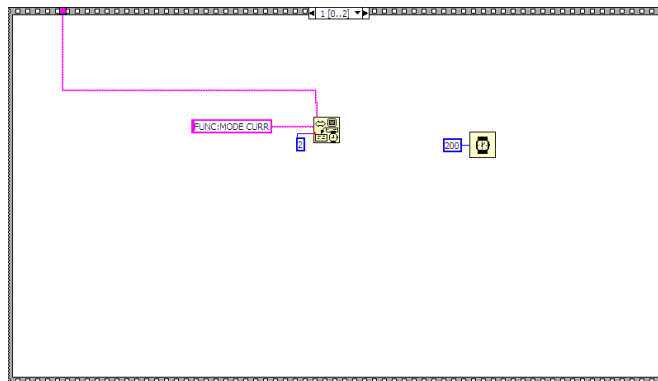
Painel principal



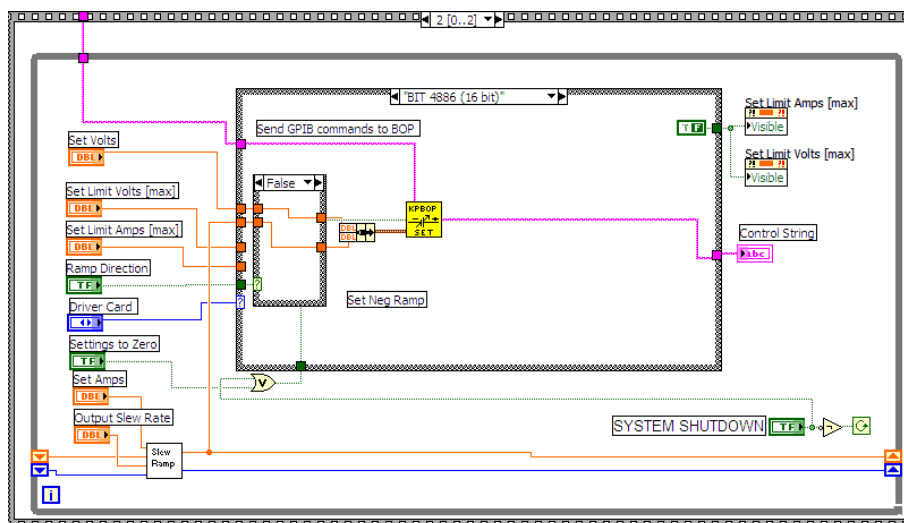
Habilitação da saída da fonte



Configuração para o modo corrente

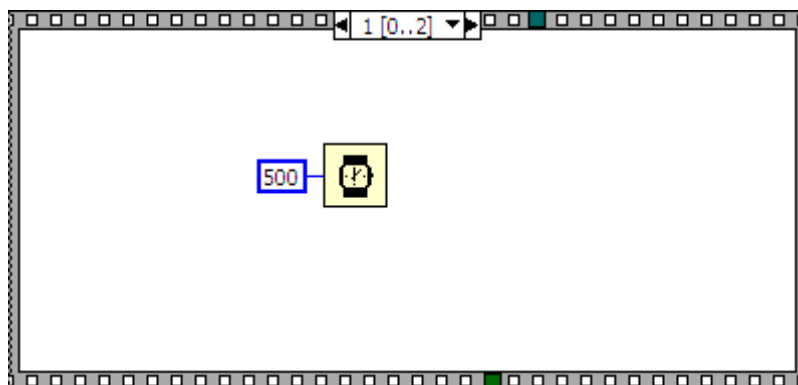
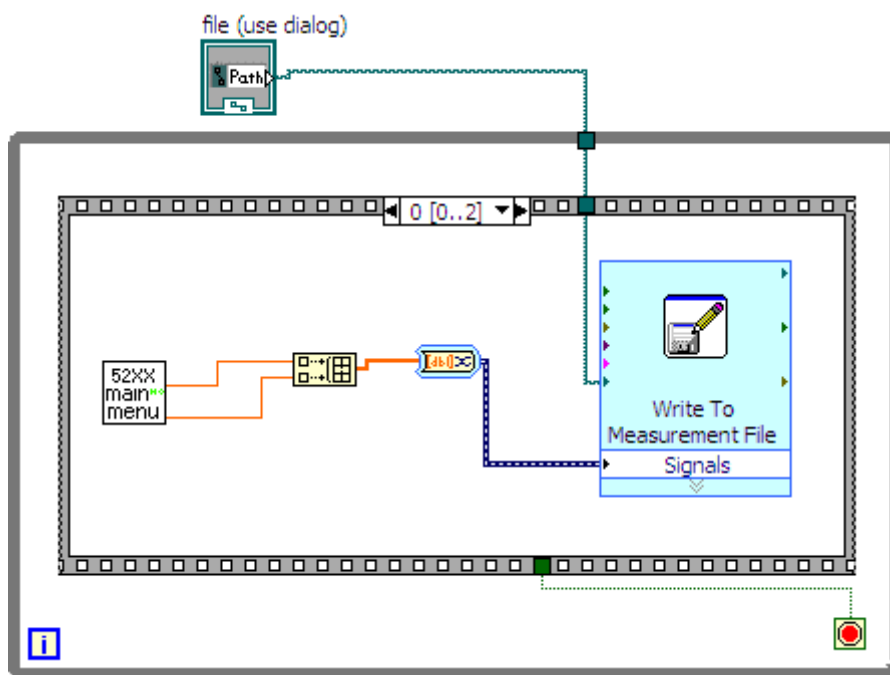
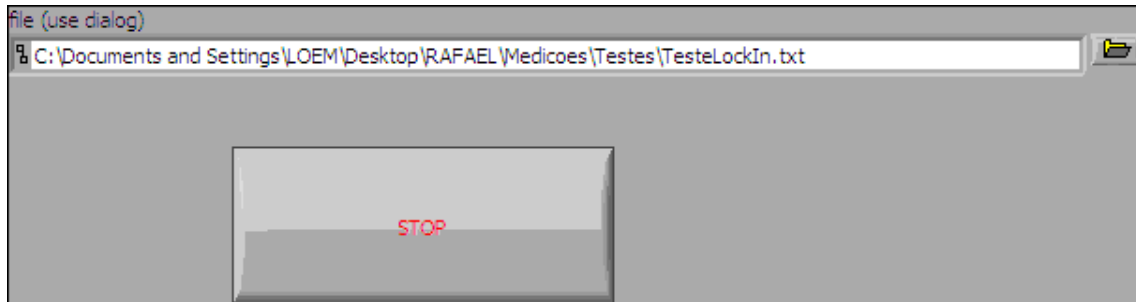


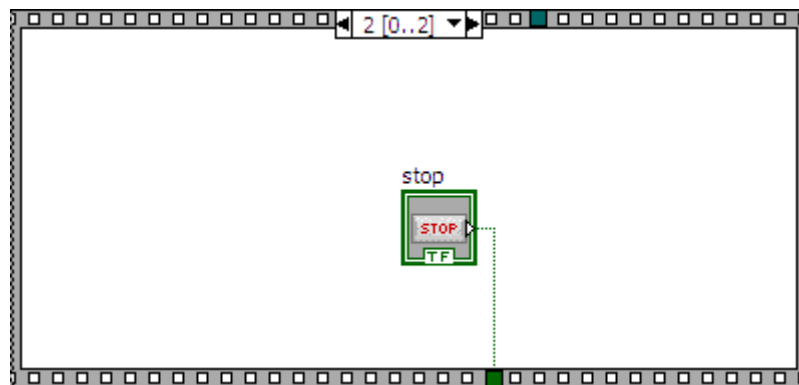
Controle da fonte



(ii) Controle do amplificador *Lock-in*.

Painel principal





Painel principal de controle da coleta dos dados de tensão do amplificador *Lock-in*

Exit
 Interface: RS232 / GPIB
 GPIB Address: 12
 Port: COM 1
 Uses VISA Communications

Model: Lock-in Amplifier Front-Panel VI

Input Configuration

Line Frequency Rejection Filter: OFF

Input Mode: Voltage Input (A or A-B)

Sensitivity Range: 1V

Buttons: Auto Sensitivity, Auto Measure

Signal Channel Filter

FilterType: Bandpass

Filter Frequency (Hz): 2

Filter Tuning: Auto

Output Channels

Time Constant: 10ms

Slope: 12dB/octave

Dynamic Reserve: Normal

Output Offset

X Channel Offset (%): 0.0

Y Channel Offset (%): 0.0

Buttons: On, Off, Auto Offset

Reference Channel

Reference Input: Unlocked

Reference Mode: 2F

Oscillator Amp (V rms): 0.500

Oscillator Freq (Hz): 1000.000

Reference Phase: 0.0

Buttons: Auto Phase, +90 degrees

Auxiliary I/O

Lights: On

Output(s)

X %

0.000 %

Y %

0.000 %

Overload

error in (no error)

status: no error, code: 0

source:

error out

status: no error, code: 0

source:

